DENSITY FUNCTIONAL STUDY OF THE ELECTRONIC STRUCTURE AND RELATED PROPERTIES OF Pt(NO)/Pt(NO_2) REDOX COUPLES

Paraskevas KARIPIDIS[1], Athanassios C. TSIPIS[2] and Constantinos A. TSIPIS[3,*]

Laboratory of Applied Quantum Chemistry, Faculty of Chemistry, Aristotle University of Thessaloniki, 540 06 Thessaloniki, Greece; e-mail: [1] paris.karipidis@mycosmos.gr, [2] a.c.tsipis@bristol.ac.uk, [3] tsipis@chem.auth.gr

Received July 24, 2002
Accepted November 1, 2002

Dedicated to Professors Petr Čársky, Ivan Hubač and Miroslav Urban on the occasion of their 60th birthdays.

Density functional calculations at the B3LYP level of theory, using the SDD basis set, provide satisfactory description of geometric, energetic, electronic and spectroscopic properties of the Pt(NO)/Pt(NO_2) redox couple. The neutral Pt(NO) species adopts a bent $^2A'$ ground state, while the cationic $[Pt(NO)]^+$ species adopts a linear $^1\Sigma^+$ ground state. The B3LYP/SDD-predicted Pt–N bond lengths are 2.016 and 1.777 Å for Pt(NO) ($^2A'$) and $[Pt(NO)]^+$ ($^1\Sigma^+$), respectively, while the ∠Pt–N–O bent angle for [Pt(NO)] ($^2A'$) is 119.6°. On the other hand, the anionic $[Pt(NO)]^-$ species adopts the bent $^1A'$ ground state with a Pt–N bond length of 1.867 Å and a ∠Pt–N–O bent angle of 122.5°. The computed binding energies of the NO, NO^+ and NO^- ligands with Pt(0) were found to be 29.9 (32.8), 69.9 (78.4) and 127.4 (128.7) kcal/mol at the B3LYP/SDD and CCSD(T)/SDD (numbers in parentheses) levels of theory, respectively. Moreover, the structure of the $[Pt(NO_2)]^+$ component of the Pt(NO)/Pt(NO_2) redox couple and its transformation to $[Pt(NO)]^+$ upon reaction with CO was analysed in the framework of the DFT theory. The coordination of the CO ligand to $[Pt(NO_2)]^+$ affords the cationic mixed-ligand $[Pt(CO)(NO_2)]^+$ complex, which is stabilized by 66.6 (60.5) kcal/mol, with respect to the separated $[Pt(NO_2)]^+$ and CO in their ground states. The O-transfer reaction from the coordinated NO_2 to the coordinated CO ligands in the presence of the $[Pt(NO_2)]^+$ species corresponds to an exothermic process; the heat of the reaction ($\Delta_R H$) is –85.2 (–80.5) kcal/mol and the activation barrier amounts to 27.7 (33.0) kcal/mol. Finally, the equilibrium structures of selected stationary points related to the transformation of NO to NO_2 ligand located on the potential energy surfaces of the $[Pt(NO),O_2]$, $[Pt(NO)^+,O_2]$, and $[Pt(NO)^-,O_2]$ systems were analysed in the framework of the DFT theory. The computed interaction energies of O_2 with Pt(NO), $[Pt(NO)]^+$ and $[Pt(NO)]^-$ species were found to be 106.9 (105.3), 49.2 (48.4) and 26.9 (26.5) kcal/mol, respectively. The O_2 ligand is coordinated to the Pt central atom in an end-on mode for $[Pt(NO),O_2]$ and $[Pt(NO)^-,O_2]$ systems and in a side-on mode for the $[Pt(NO)^+,O_2]$ system. The transformation of NO to NO_2 in $[Pt(NO)]^-$ species upon reaction with dioxygen corresponds to an exothermic process; the heat of the reaction ($\Delta_R H$) is –60.6 (–55.8) kcal/mol, while the activation barrier amounts to 35.5 (30.2) kcal/mol. Calculated structures, relative stability and bonding properties of all stationary

points are discussed with respect to computed electronic and spectroscopic properties, such as charge density distribution and harmonic vibrational frequencies.
Keywords: DFT; Nitrosylplatinum; Nitroplatinum; Redox couple; Electronic structure; *Ab initio* calculations.

The chemistry of transition metal coordination compounds containing the nitrosyl (NO) ligand has seen a tremendous revival since the discovery[1] of NO as an essential biological molecule[2]. More recent is the interest in nitrosyl complexes as drugs that release the neurotransmitter and mammalian bioregulator NO (ref.[3]) as model complexes for metal enzymes such as nitrile hydrase[4], cytochrome oxidase[5] and nitrogenase[6], and as a potential waste gas purification catalyst[7]. Catalytic cycles involving alkali[8] and alkaline earth[9] metals have been proposed for the destruction of NO in combustion exhaust gases. The NO ligand can act as diamagnetic, strongly π-accepting NO^+, as equally diamagnetic NO^-, or as paramagnetic, neutral NO. As a consequence, specific electronic, structural, and reactivity features of the transition metal nitrosyl complexes have aroused interest since the early days of coordination chemistry. The timely and important areas of NO chemistry, from physical and computational studies to the biological role in living systems, have exhaustively been covered by a number of review articles published in a very recent issue of *Chemical Reviews*[10] devoted to NO chemistry. A variety of ···M–NO, or ···M–NO^+ type of complexes, where M = metal, have recently been studied, using the density functional theory (DFT) at various levels[11–18], but surprisingly enough, the number of *ab initio* studies is very limited[19–22] and not systematic enough. The goal of this work is to understand the possible bonding modes (bent, linear and bridging) of the nitrosyl ligand coordinated to Pt metal centers, and explore the structure, properties and thermodynamics of the Pt(NO)/Pt(NO_2) redox couple related to the intimate mechanism of the catalytic function in O-transfer reactions.

COMPUTATIONAL

Structural, electronic and energetic properties of all compounds were computed at the Becke's 3-Parameter hybrid functional[23] combined with the Lee–Yang–Parr correlation functional[24] abbreviated as the B3LYP level of theory, using the SDD basis set that includes Dunning/Huzinaga valence double-zeta on the first-row atoms and Stuttgart/Dresden ECPs on the platinum atom. Control calculations were also carried out for simple Pt–NO tri-

atomic systems using the LANL2DZ basis set[25] that includes Dunning/Huzinaga full DZ on first-row atoms and Los Alamos ECPs plus DZ for platinum atom as well as using the compact effective potential (CEP) basis functions with ECP triple-split basis, namely CEP-121G [26–28]. The hybrid B3LYP functional was used, since it gives acceptable results for molecular energies and geometries as well as for proton donation and weak and strong H-bonds[29]. In all computations no constraints were imposed on the geometry. Full geometry optimization was performed for each structure using Schlegel's analytical gradient method[30], and the attainment of the energy minimum was verified by calculating the vibrational frequencies that result in the absence of imaginary eigenvalues. All stationary points have been identified as minima (number of imaginary frequencies NIMAG = 0) or transition states (NIMAG = 1). Furthermore, to check the reliability of the B3LYP/SDD results, single-point energy calculations were performed at the CCSD(T) level using the SDD basis set. For most of the cases, the CCSD(T)/SDD results were in satisfactory agreement with the B3LYP ones (deviations range from 1 to 15%). All calculations were performed using the GAUSSIAN98 series of programs[31]. Moreover, the qualitative concepts and the graphs derived from Chem3D program suite[32] highlight the basic interactions resulting from the DFT calculations.

RESULTS AND DISCUSSION

Preliminary Studies of the Equilibrium Geometry, Electronic Structure and Bonding Mechanism of Neutral Pt(NO), Cationic $[Pt(NO)]^+$ and Anionic $[Pt(NO)]^-$ Model Compounds

To assess the ability of B3LYP and particularly the quality of basis sets used to successfully model the Pt–NO bonding and related properties in the nitrosyl complexes of Pt(II) we looked first at the NO molecule and its interactions with Pt and Pt^+ in the simple triatomic Pt(NO), $[Pt(NO)]^+$ and $[Pt(NO)]^-$ systems.

There are three geometries possible for NO binding to a bare Pt atom: linear, bent and side-on. NO has a $^2\Pi$ ground state, and thus when a Pt atom interacts with a NO molecule, the state can split into a $^2A'$ and a $^2A''$ state, depending on whether the unpaired electron is in-plane or out-of-plane. In the linear η^1-NO bonding mode, the NO ligand is bound to the Pt atom *via* a donor σ bond, comprising of the N lone pair delocalizing into an empty metal σ orbital and a covalent π bond, formed from the unpaired 2π electron (primarily N 2p) and a metal d electron (Fig. 1a). Here we have a "har-

poon-like" bond of σ character and a second bond of π character. In the bent η^1-NO bonding mode of C_s symmetry, the NO ligand utilizes its 2π unpaired electron and a metal σ electron to form a covalent σ bond, leaving the 5σ or N 2s lone pair non-bonding (Fig. 1b). In the side-on bonding mode of NO to Pt atom one would expect a drastic change in the character of the orbitals of Pt(NO) and $[Pt(NO)]^+$ species. The 1a′ orbital is a σ-type bonding MO formed from the in-plane, formerly d_π orbital, interacting with both the nitrogen and oxygen components of the in-plane π* orbital of NO. The out-of-plane d_π orbital forms a π-type bond, 1a″, with the out-of-plane NO π* orbital (Fig. 1c). The NO ligand could also act as a bridging ligand. In the μ-NO bonding mode, the 5σ lone pair and the unpaired

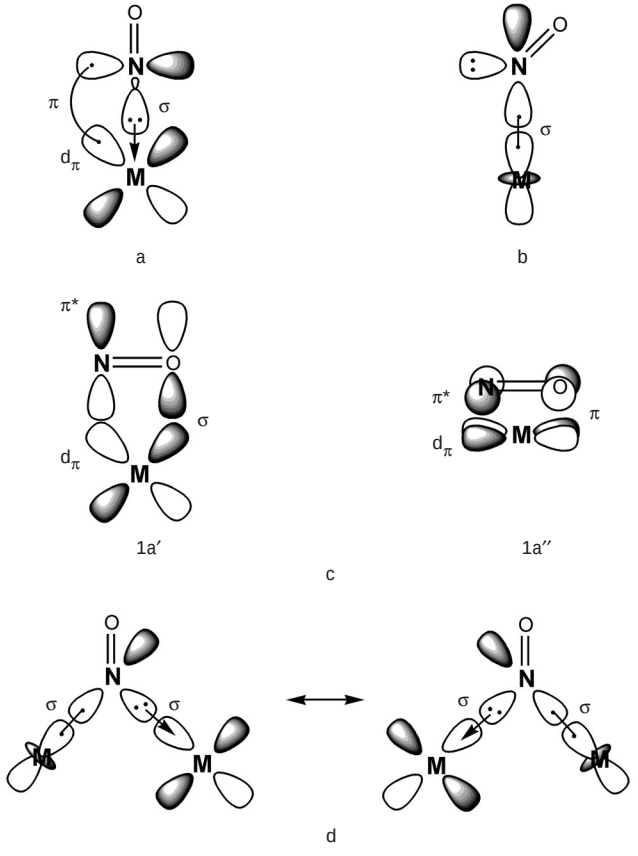

FIG. 1
Qualitative depiction of bonding between NO and a Pt atom: linear $^2\Sigma^+$ Pt(NO) (a); bent ^{2}A″ or ^{2}A′ end-on Pt(NO) (b); ^{2}A″ side-on Pt(NO) (c); bridging Pt(μ-NO) (d)

2π electron are used respectively to form a coordination σ bond to one metal atom and a covalent σ bond to another metal atom. In effect, the actual bonds are a linear combination of two resonance structures (Fig. 1d).

The computed geometric, energetic and spectroscopic properties of the NO ligand at the B3LYP level of theory using three different basis sets are summarized in Table I and are compared with previously reported theoretical data and experiment. It can be seen that both SDD and LANL2DZ basis sets give identical results which are in close agreement with the GVB(3/6)-PP [21] and experimental data[33]. The predicted N–O bond length at the B3LYP/SDD and B3LYP/LANL2DZ levels of theory is 0.048 Å longer than that observed experimentally[33], while the predicted harmonic vibrational frequencies are within 7% of the experimental value[33]. The predicted value of 0.093 D for the dipole moment of NO at both the B3LYP/SDD and B3LYP/LANL2DZ levels is in excellent agreement with *ab initio* calculations of Walch and Goddard[34], which predict a value of 0.10 D, but it is significantly smaller than the experimental value of 0.153 D. The B3LYP/CEP-121 value, 0.139 D, is much closer to the experimental value, but still slightly too small.

Pt has a ^{3}D ground state, which suggests that linear $^2\Sigma^+$ or bent ^{2}A′ (or ^{2}A″) PtNO structures could be adopted. Indeed, we find the bent ^{2}A′ state to be the global minimum in the potential energy surface (PES) of Pt(NO) for all basis sets used. The calculated properties of Pt(NO) states at the B3LYP

TABLE I
Calculated properties of NO ($^2\Pi$) at the B3LYP level using the SDD, LANL2DZ and CEP-121 basis sets

Parameter	SDD	LANL2DZ	CEP-121	GVB(3/6)-PP [a]	Expt
E (E_h)	–129.85698	–199.85627	–25.74650	–129.32958	–
R_e(N–O), Å	1.199	1.199	1.208	1.157	1.151[b]
ω_e(NO), cm^{-1}	1771.4	1770.5	1756.6	1813.4	1904.2[b]
μ_e, D	0.093	0.093	0.139	0.017	0.153[c]
q_N[d,e]	0.20 (0.07)	0.20 (0.07)	0.21 (0.02)	–	–
q_O[d,e]	–0.20 (–0.07)	–0.20 (–0.07)	–0.21 (–0.02)	–	–
BOP[f]	0.217	0.206	0.128	–	–

[a] Ref.[32]. [b] Ref.[33]. [c] Ref.[34]. [d] Natural charges. [e] Numbers in parentheses are the Mulliken net atomic charges. [f] Mulliken bond overlap population.

level using the three different basis sets are summarized in Table II. In general terms, the predicted properties of the $^2A'$ ground state of Pt(NO) using the SDD basis set are in close agreement with those computed using the CEP-121 basis sets, but differ significantly from those computed with the LANL2DZ basis set. The computed B3LYP/SDD and B3LYP/CEP-121 properties for the $^2A'$ ground states of Pt(NO) are also consistent with those of the $^2A'$ ground state computed at the GVB-PP level of theory[21]. Thus, the equilibrium bond angle of 119.6 and 119.3° using the SDD and CEP-121 basis sets, respectively, is in close agreement with the GVB-PP value of 112.9°. Similarly, the predicted B3LYP/SDD and B3LYP/CEP-121 equilibrium Pt–N bond lengths of 2.016 and 2.024 Å, respectively, are in better agreement with the GVB-PP value[21] of 2.16 Å than the B3LYP/LANL2DZ value of 1.832 Å. This is also reflected in the computed binding energies, which were found to be 29.9, 24.7 and 52.9 kcal/mol using the SDD, CEP-121 and LANL2DZ basis sets, respectively. It is worth noting that the predicted binding energies at the B3LYP/SDD and B3LYP/CEP-121 levels are in good agreement with the GVB-PP value of 20.4 kcal/mol. Finally the ω_e(PtN–O) vibrational frequencies of 1771, 1769 and 1757 cm^{-1} computed at the B3LYP/SDD, B3LYP/LANL2DZ and B3LYP/CEP-121 levels, respectively, are in good agreement with the experimental value of 1712.6 cm^{-1} in solid neon matrix[35].

The sequence of Kohn–Sham molecular orbitals (MOs) deduced for the $^2A'$ ground state of Pt(NO) using, respectively, the SDD, CEP-121 and LANL2DZ basis sets is

$\cdots(9a')^2(3a'')^2(4a'')^2(10a')^2\ (11a')^2(12a')^2(13a')^1$

$\cdots(7a')^2(3a'')^2(4a'')^2(8a')^2(9a')^2(10a')^2(11a')^1$ and

$\cdots(2a'')^2(10a')^2(3a'')^2(11a')^2\ (4a'')^2(12a')^2(13a')^1$.

The SOMO (singly occupied molecular orbital) of a′ at –6.516, –6.479 and –6.436 eV using the SDD, CEP-121 and LANL2DZ basis sets, respectively, corresponds to a σ-type Pt–N bond resulting from the interaction of the polarized 6s orbital of the Pt atom with the out-of-plane NO π* orbital (Fig. 2a). On the other hand, the 5a″ LUMO (lowest unoccupied molecular orbital) at –3.840, –3.759 and –3.727 eV using the SDD, CEP-121 and LANL2DZ basis sets, respectively, corresponds to a π-type Pt–N bond resulting from the interaction of an out-of-plane d_π orbital of the Pt atom with the out-of-plane NO π* orbital. Depending on the basis set used, the total atomic spin density of the $^2A'$ ground state is either mainly located on the central Pt atom (≈1.17) and much less on the N-donor atom (≈ –0.09) (Fig. 2b) or it is delocalised over the entire nuclear skeleton, with the Pt, N and O atoms acquiring 0.411, 0.340 and 0.250 spin densities, respectively (Fig. 2c).

TABLE II
Calculated properties of Pt(NO) states at the B3LYP level using the SDD, LANL2DZ and CEP-121 basis sets

Parameter	SDD		LANL2DZ		CEP-121	
	$^2A'$	$^2\Sigma^+$	$^2A'$	$^2\Sigma^+$	$^2A'$	$^2\Sigma^+$
E (E_h)	–249.20672	–249.20660	–249.01763	–248.97767	–145.48771	–145.41789
ΔE, kcal/mol	0.0	0.1	0.0	25.1	0.0	unbound
D_e(Pt–NO), kcal/mol	29.9	29.8	52.9	27.8	24.7	unbound
R_e(Pt–NO), Å	2.016	1.807	1.832	1.813	2.024	4.162
R_e(PtN–O), Å	1.220	1.193	1.217	1.192	1.232	1.207
θ_e(Pt–N–O), °	119.6	180.0	134.9	180.0	119.3	180.0
ω_e(Pt–NO), cm^{-1}	304	504	290	503	305	16*i*
ω_e(PtN–O), cm^{-1}	1558	1771	1623	1769	1539	1757
ω_e(Pt–N–O bend), cm^{-1})	558	978	613	948	552	20
μ_e, D	1.17	1.58	1.78	1.81	1.31	0.04
q_{Pt} [a,b]	0.16 (0.07)	0.09 (0.04)	0.15 (0.17)	0.09 (0.11)	0.17 (0.03)	–0.00 (–0.01)
q_N [b]	0.03 (0.01)	0.02 (–0.01)	0.03 (–0.08)	0.02 (–0.08)	0.03 (0.00)	0.21 (0.02)
q_O [b]	–0.19 (–0.08)	–0.11 (–0.03)	–0.18 (–0.09)	–0.11 (–0.02)	–0.20 (–0.04)	–0.21 (–0.01)
BOP(Pt–NO) [c]	0.208	0.070	0.225	0.127	0.261	0.012
BOP(PtN–O)	0.211	0.253	0.225	0.229	0.129	0.112

[a] Natural charges. [b] Numbers in parentheses are the Mulliken net atomic charges. [c] Mulliken bond overlap population.

According to the natural bond orbital (NBO) and Mulliken population analyses (Table II), there is a significant charge transfer of about 0.17 charge units of natural charge from Pt to the N-donor atom of Pt(NO) molecule at both the B3LYP/SDD and B3LYP/CEP-121 levels of theory. In contrast, the Mulliken population analysis predicts a small net charge transfer from Pt to the N-donor atom amounting to 0.07 and 0.03 charge units at the B3LYP/SDD and B3LYP/CEP-121 levels of theory, respectively. The predicted metal-to-ligand charge transfer results in the weakening of the N–O bond (*cf.* the bond overlap populations of the free and coordinated NO ligands), because electron density is accumulated on the antibonding π*-MO of the coordinated NO ligand.

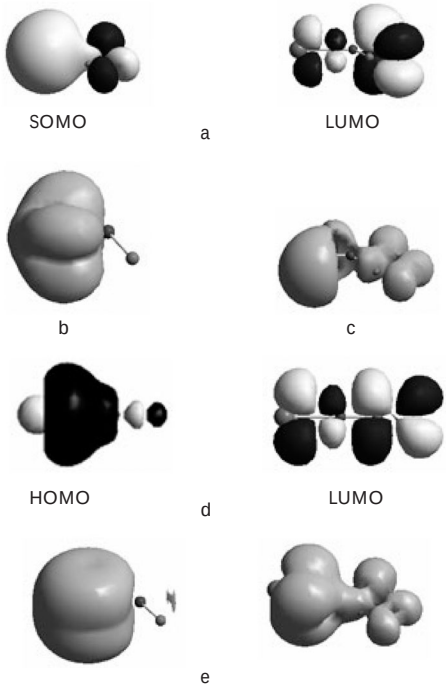

FIG. 2

The singly occupied (SOMO) and lowest unoccupied (LUMO) molecular orbitals of the $^2A'$ ground state of Pt(NO) (a) along with the atomic spin densities (isospin surface of 0.002 a.u.) computed at the B3LYP/SDD (b) and B3LYP/LANL2DZ (c) levels of theory, respectively. The highest occupied (HOMO) and LUMO of the linear $^1\Sigma^+$ ground state of $[Pt(NO)]^+$ (d) along with the atomic spin densities (isospin surface of 0.002 a.u.) computed at the B3LYP/SDD and B3LYP/LANL2DZ levels of theory (e), respectively

Pt^+ in its ^2D ground state having only d valence electrons would be expected to stabilize the linear $^1\Sigma^+$ state in the $[Pt(NO)]^+$ cationic species. In effect, we find the linear $^1\Sigma^+$ state to be the global minimum in the PES of $[Pt(NO)]^+$ at the B3LYP/SDD and B3LYP/LANL2DZ levels of calculations, but roughly bent (174.3°) at the B3LYP/CEP-121 level. On the other hand, in the excited triplet state $[Pt(NO)]^+$ adopts the bent $^3A'$ configuration. At the B3LYP/CEP-121 level, the excited bent $^3A'$ configuration was predicted to be unbound. In contrast to the predictions of the DFT theory that the $[Pt(NO)]^+$ cationic species exhibits the linear $^1\Sigma^+$ as the ground state at the B3LYP level, the GVB(4/8)-PP level[21] predicts the bent $^1A'$ configuration as the ground state with the linear $^1\Sigma^+$ state about 13 kcal/mol above the bent $^1A'$ ground state. However, all M–NO^+ species for M = Cr–Ni were recently[11] predicted to adopt the linear $^1\Sigma^+$ as the ground state at the DFT level of theory. The calculated properties of $[Pt(NO)]^+$ states at the B3LYP level using the three different basis sets are summarized in Table III. Generally, the predicted properties of the linear $X^1\Sigma^+$ ground states of $[Pt(NO)]^+$ cationic species using the SDD basis set are in close agreement with those computed using the LANL2DZ basis sets, but differ significantly from those of the $^1A'$ ground state computed with the CEP-121 basis set. The computed binding energies, found to be 69.9 and 68.9 kcal/mol using the SDD and LANL2DZ basis sets, respectively, compare well with the binding energies of 46.75 and 49.26 kcal/mol computed at the CCSD(T)AW/cc-pVTZ and CCSD(T)AANO/cc-pVTZ levels for the $^1\Sigma^+$ ground state of $[Ni(NO)]^+$ species[11]. In contrast, the predicted binding energy of 24.7 kcal/mol for the $^1A'$ ground state of $[Pt(NO)]^+$ computed at the B3LYP/CEP-121 level seems to be too low. The computed binding energies, being higher in the $[Pt(NO)]^+$ than in the neutral Pt(NO) species, strongly suggest that upon ionization the Pt–N bond becomes stronger as expected for a linearly coordinated NO^+ ligand. This is also reflected in the computed Pt–N bond lengths, which are shorter in the $[Pt(NO)]^+$ species by 0.24, 0.06 and 0.24 Å using the SDD, LANL2DZ and CEP-121 basis sets, respectively. The shortening of the Pt–N bond is also accompanied by a shortening of the N–O bond by 0.06, 0.05 and 0.06 Å using the SDD, LANL2DZ and CEP-121 basis sets, respectively, as expected for a NO^+ ligand. Finally the ω_e(Pt–NO) and ω_e(PtN–O) vibrational frequencies of 169 and 1949 cm^{-1}, respectively, computed at the B3LYP/SDD level are in quite good agreement with the corresponding vibrational frequencies of 189 and 2013 cm^{-1} for the $^1\Sigma^+$ state of $[Pt(NO)]^+$ computed at the GVB(4/8)-PP level[21]. The experimental value of the ω_e(PtN–O) vibrational frequency in solid neon matrix[35] is 2019.6 cm^{-1}.

TABLE III
Calculated properties of $[Pt(NO)]^+$ states at the B3LYP level using the SDD, LANL2DZ and CEP-121 basis sets

Parameter	SDD		LANL2DZ		CEP-121	
	$^1\Sigma^+$	$^3A'$	$^1\Sigma^+$	$^3A'$	$^1\Sigma^+$	$^3A'$
E (E_h)	–248.92935	–248.81620	–248.70022	–248.65679	–145.20991	–145.41789
ΔE, kcal/mol	0.0	71.0	0.0	27.3	0.0	unbound
D_e(Pt–NO), kcal/mol	69.9	–	68.9	–	24.7	–
R_e(Pt–NO), Å	1.777	2.711	1.773	1.986	1.783	2.726
R_e(PtN–O), Å	1.162	1.163	1.163	1.180	1.173	1.175
θ_e(Pt–N–O), °	180.0	121.5	180.0	133.0	174.3	121.3
ω_e(Pt–NO), cm^{-1}	169	104	208	270	70	100
ω_e(PtN–O), cm^{-1}	1949	1828	1950	1778	1907	1788
ω_e(Pt–N–O bend), cm^{-1})	554	300	567	430	553	290
μ_e, D	0.25	2.29	0.24	0.15	0.18	1.96
q_{Pt} [a,b]	0.75 (0.78)	0.64 (0.62)	0.77 (0.85)	0.87 (0.85)	0.77 (0.77)	0.72 (0.68)
q_N [a,b]	0.18 (0.06)	0.32 (0.24)	0.16 (–0.004)	0.09 (0.02)	0.16 (–0.06)	0.28 (0.12)
q_O [b]	0.08 (0.16)	0.04 (0.15)	0.07 (0.16)	0.04 (0.13)	0.05 (0.29)	–0.003 (0.20)
BOP(Pt–NO)[c]	0.196	0.091	0.142	0.138	0.239	0.083
BOP(PtN–O)	0.343	0.275	0.343	0.256	0.297	0.172
IP, eV	7.55	–	8.64	–	7.56	–

[a] Natural charges. [b] Numbers in parentheses are the Mulliken net atomic charges. [c] Mulliken bond overlap population.

The sequence of Kohn–Sham molecular orbitals (MOs) deduced for the $X^1\Sigma^+$ state of $[Pt(NO)]^+$ using the SDD and LANL2DZ basis sets is $\cdots(3\pi)^4(1\delta)^4(8\sigma)^2$, while that of the $^1A'$ ground state computed with the CEP-121 basis set is $\cdots(3a'')^2(10a')^2(4a'')^2(11a')^2(12a')^2$. The HOMO (highest occupied molecular orbital) of σ(a′) symmetry at –14.476, –14.526 and –14.432 eV using the SDD, LANL2DZ and CEP-121 basis sets, respectively, corresponds to a σ-type Pt–N bond resulting from the interaction of the polarized 6s orbital of the Pt atom with the out-of-plane NO π* orbital (Fig. 2d). On the other hand, the LUMO (lowest unoccupied molecular orbital) of π(a′) symmetry at –10.440, –10.651 and –10.613 eV using the SDD, LANL2DZ and CEP-121 basis sets, respectively, corresponds to a π-type Pt–N bond resulting from the interaction of an out-of-plane d_π orbital of the Pt atom with the out-of-plane NO π* orbital. In the bent $^3A'$ excited state, the total atomic spin density (Fig. 2e) is mainly located on the central Pt atom, the computed values being 2.58 and 1.29 using the SDD and LANL2DZ basis sets, respectively, and much less on the N-donor atom (–0.36 and 0.40 using the SDD and LANL2DZ basis sets, respectively) and on the O atom (–0.22 and 0.31 using the SDD and LANL2DZ basis sets, respectively).

According to the natural bond orbital (NBO) and Mulliken population analyses (Table III), there is a significant charge transfer of about 0.23–0.27 charge units of natural charge from the NO ligand to Pt^+ ion, while concomitantly both the N-donor and O atoms lose 0.13–0.15 and 0.25–0.27 charge units of natural charge, respectively. The predicted ligand-to-metal charge transfer results in the strengthening of the N–O bond (*cf.* the bond overlap populations of the free and coordinated NO ligand), because electron density is accumulated on the bonding π-MO of the coordinated NO ligand. At all levels of theory, the NBO analysis assigns a $6s^{0.38}5d^{8.87}$, $2s^{1.55}2p^{3.21}$ and $2s^{1.75}2p^{4.16}$ population to Pt, N and O atoms in the $X^1\Sigma^+$ state of NO. On the other hand, the NBO analysis assigns a $6s^{1.40}5d^{7.95}$, $2s^{1.74}2p^{2.89}$ and $2s^{1.77}2p^{4.17}$ population to Pt, N and O atoms in the bent $^3A'$ excited state of $[Pt(NO)]^+$ species at the B3LYP/SDD level of theory. Note that the total natural populations on the Pt, N and O atoms, being 9.25, 6.82 and 7.92, respectively, are in excellent agreement with those computed at the GVB(4/8)-PP level[21].

According to our preliminary studies it can be concluded that the quality of the basis sets used is important to successfully model the Pt–NO bonding and related properties in the nitrosyl complexes of Pt(II). A thorough inspection of the results reveals that the SDD basis set models better most of the properties of the Pt(NO) systems and, therefore, we decided to use this basis set in our study of the more complex Pt(II) nitrosyl complexes.

Finally, the geometric, energetic and spectroscopic properties of the singlet (ground) and triplet (excited) state of the anionic $[Pt(NO)]^-$ species have been computed at the B3LYP/SDD level of theory and the results are summarized in Table IV. It was found that the singlet $^1A'$ state is the global minimum in the PES of $[Pt(NO)]^-$ species with the excited triplet $^3A'$ state being about 96 kcal/mol higher in energy. Both states adopt the bent structures, the bending angles being 122.5 and 125.0° for the $^1A'$ and $^3A'$ states, respectively. The predicted binding energies with respect to $Pt(^3D)$ and NO^- ground states are 127 and 32 kcal/mol for the $^1A'$ and $^3A'$ states, respectively. The higher Pt–N bond dissociation energy of the anionic species with respect to that of the neutral and cationic species strongly suggests that the extra electron contributes to the covalent σ bond between Pt and NO. This is mirrored in both the computed Pt–N bond lengths and the ω_e(Pt–NO) vibrational frequencies. The computed ω_e(PtN–O) vibrational frequency of 1384 cm^{-1} for the $^1A'$ ground state of $[Pt(NO)]^-$ species is in good

TABLE IV
Calculated properties of the $[Pt(NO)]^-$ states at the B3LYP/SDD level

Parameter	$^1A'$	$^3A'$
E (E_h)	–249.32625	–249.17379
ΔE, kcal/mol	0.00	95.66
D_e(Pt–NO), kcal/mol	127.4	31.70
R_e(Pt–NO), Å	1.867	2.595
R_e(PtN–O), Å	1.265	1.296
θ_e(Pt–N–O), °	122.5	125.0
ω_e(Pt–NO), cm^{-1}	348.4	78.0
ω_e(PtN–O), cm^{-1}	1384.3	1292.8
ω_e(Pt–N–O bend), cm^{-1}	679.8	195.7
μ_e, D	1.49	4.72
$q_{Pt}{}^{a,b}$	–0.55 (–0.65)	–0.15 (–0.43)
$q_N{}^{a,b}$	–0.06 (–0.08)	–0.42 (–0.22)
$q_O{}^{a,b}$	–0.39 (–0.27)	–0.43 (–0.35)
BOP(Pt–NO)[c]	0.270	0.160
BOP(PtN–O)	0.178	0.110

[a] Natural charges. [b] Numbers in parentheses are the Mulliken net atomic charges. [c] Mulliken bond overlap population.

agreement with the experimental value of 1462.1 cm^{-1} in solid neon matrix[35,36]. According to the natural bond orbital (NBO) and Mulliken population analyses (Table IV), there is a significant charge transfer of about 0.55 (0.65) and 0.15 (0.430) charge units of natural, net-atomic charge from the N-donor atom to Pt for the $^1A'$ and $^3A'$ states of $[Pt(NO)]^-$ species, respectively. The predicted ligand-to-metal charge transfer results in strengthening of the Pt–N and the weakening of the N–O bonds. The NBO analysis assigns a $6s^{1.55}5d^{8.93}6s^{0.07}$ and $6s^{1.94}5d^{7.99}6s^{0.07}$ natural electron configuration of Pt atom for the $^1A'$ and $^3A'$ states of $[Pt(NO)]^-$ species, respectively.

The $[Pt(NO_2)]^+$ Component of the Pt(NO)/Pt(NO_2) Redox Couple and Its Transformation to $[Pt(NO)]^+$ upon Reaction with CO

Another goal of this work is the study of the oxygen carrier component of the Pt(NO)/Pt(NO_2) redox couple, namely the $[Pt(NO_2)]^+$ species **1**, and its reverse transformation to the $[Pt(NO)]^+$ component upon reaction with CO resulting in the oxidation of CO to CO_2. The energetic and geometric profile of the reaction of $[Pt(NO_2)]^+$ with CO is depicted schematically in Fig. 3. The coordination of the CO ligand to $[Pt(NO_2)]^+$ affords the mixed-ligand carbonylnitroplatinum complex **2**, being stabilized by 66.6 (57.9) kcal/mol, with respect to the separated $[Pt(NO_2)]^+$ and CO species in their ground states. This value corresponds to the binding energy of the CO ligand to the $[Pt(NO_2)]^+$ metal-containing fragment. Noteworthy is the V-type (bent) coordination in **2**, the ∠N–Pt–O bond angle being equal to 115.0°. Moreover, the NO_2 ligand seems to adopt a η^2-O,N coordination bond with the Pt–N and Pt–O bond distances being 1.299 and 2.265 Å, respectively. In complex **2**, an intramolecular O-migration from the NO_2 to CO ligand occurs *via* the transition state **TS1** affording the mixed-ligand (carbon dioxide)nitrosylplatinum complex **3** with the CO_2 molecule coordinated to the central Pt atom in a η^1-OCO bonding mode. In contrast to $[Pt(CO)(NO_2)]$, the $[Pt(CO_2)(NO)]$ complex adopts a N–Pt–C linear configuration with the coordinated CO_2 ligand deviated from linearity by only 6°. The computed interaction energy of the CO_2 molecule with $[Pt(NO)]^+$ was predicted to be 37.3 (37.2) kcal/mol. In summary, the oxidation of CO to CO_2 in the presence of the $[Pt(NO_2)]^+$ species corresponds to an exothermic process; the heat of the reaction is –85.2 (–80.5) kcal/mol and the activation barrier is 27.7 (33.0) kcal/mol. In **TS1**, the coordinated CO ligand approaches the O atom of the NO_2 ligand forming a cyclic transition state involving a planar four-membered metallacycle ring. The imaginary frequency of **TS1** ν_i = 371 cm^{-1} corresponds to the stretching of the Pt–CO bond with concomitant bend-

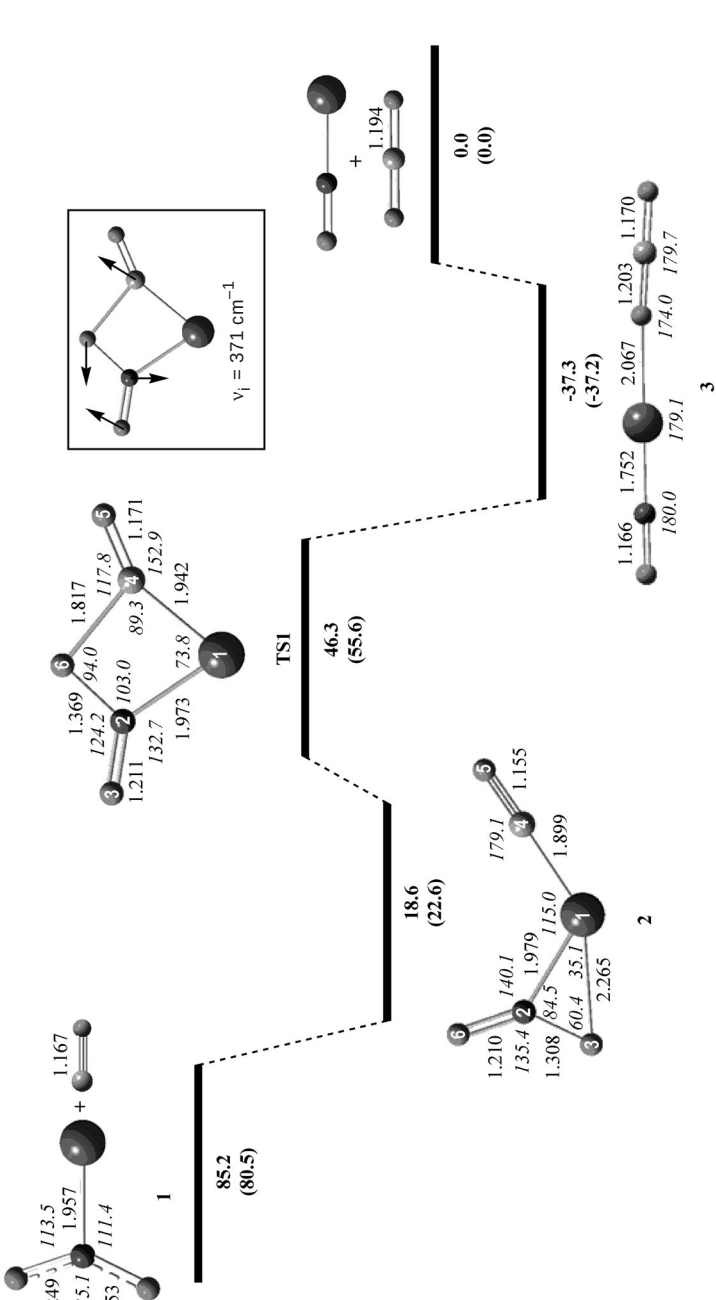

FIG. 3

The energetic and geometric profile of the intramolecular O-transfer reaction from the NO_2 ligand to CO in the cationic mixed-ligand $[Pt(CO)(NO_2)]^+$ complex (energies are given in kcal/mol) computed at the B3LYP/SDD level of theory. Numbers in parentheses are the energies computed at the CCSD(T)/SDD level of theory

ing of the ONO group. The normal coordinate vectors (arrows) of the vibrational mode are shown in Fig 3. In **TS1**, the C–O and one of the N–O bonds including the O atom to be transferred are lengthened by 0.02 and 0.06 Å, respectively, while there is a strong bending of the ∠Pt–C–O bond angle by about 26°. Moreover, there is a remarkable lengthening of the Pt–C bond amounting to 0.04 Å. Finally, upon coordination of the CO ligand to Pt atom of the $[Pt(NO_2)]^+$ fragment, there is a significant charge transfer of about 0.16 charge units of net atomic charge from the CO ligand to Pt central atom, while the Pt–N bond is lengthened by 0.02 Å. In **TS1**, 0.05 charge units are transferred back to the CO ligand because of its intramolecular interaction with the O atom of the NO_2 ligand being migrating to CO ligand.

Let us now go deeper into the orbital interactions along the reaction pathway of the O-transfer reaction. The frontier molecular orbitals (FMOs) of all species involved in the O-transfer reaction are shown in Fig. 4. It can be seen that the LUMO of the $[Pt(NO_2)]^+$ species being primarily localized on the Pt central atom could interact with the σ-type donor MO of CO to

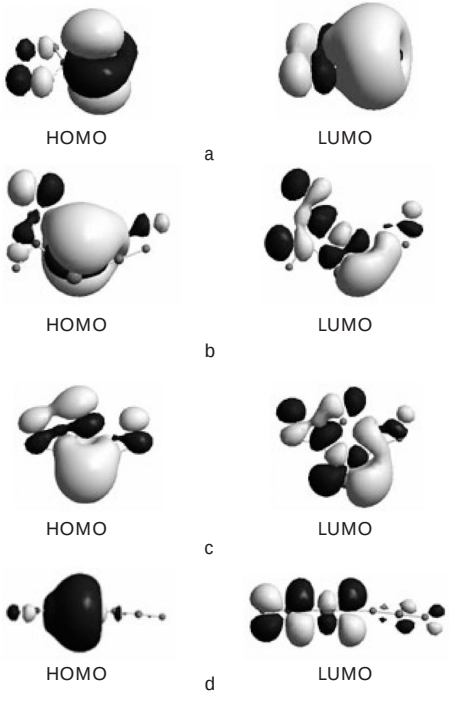

FIG. 4

The HOMO and LUMO of all species involved in the intramolecular O-transfer reaction from the NO_2 ligand to CO in the cationic mixed-ligand $[Pt(CO)(NO_2)]^+$ complex

form a σ-coordination Pt←CO bond. Because of the cylindrical symmetry of the LUMO, the interaction leads to a bending N–Pt–C coordination mode, the bending angle being 115.0°. Moreover, the HOMO of the $[Pt(NO_2)]^+$ species, being also localized on the Pt central atom, could interact with the π*-MO of the CO ligand, thus forming a π-back bond. This is reflected in the nature of the HOMO of species **2**, which is a π-MO localized on the Pt–C bond (Fig. 4). The HOMO of the transition state **TS1** is similar to that of species **2**, but with a slight polarization towards the migrating O atom of the NO_2 ligand. Finally, the HOMO of complex **3** resembles that of the linear $^1\Sigma^+$ state of the $[Pt(NO)]^+$ cationic species, but involving weak bonding interactions with the appropriate σ-MO of the CO_2 ligand corresponding to a σ-coordination Pt←O bond. Upon the formation of the σ-coordination Pt←O=C=O bond, electron density is transferred towards the Pt central atom, which brings a consequence of weakening the adjacent C=O bond of the coordinated CO_2 ligand (*cf.* C–O bond lengths of 1.203 and 1.170 Å). The HOMO-LUMO energy gap for the isomeric compounds **2**, **TS1** and **3**, being 3.59, 3.44 and 3.82 eV, respectively, reflect relative stability of the compounds.

Interaction of the Pt(NO), $[Pt(NO)]^+$ and $[Pt(NO)]^-$ Species with Dioxygen

Let us now explore the potential energy surfaces of the $[Pt(NO),O_2]$, $[Pt(NO)^+,O_2]$, and $[Pt(NO)^-,O_2]$ systems. The equilibrium structures of selected stationary points related to the transformation of the NO to NO_2 ligand located on the PES of the $[Pt(NO),O_2]$ system are depicted schematically in Fig. 5. The interaction of the neutral Pt(NO) species with dioxygen in its triplet ground state affords complex **4** in a doublet ground state with the dioxygen ligand being coordinated to the central Pt atom in a side-on bonding mode. The computed interaction energy was found to be 106.9 (105.3) kcal/mol. Upon coordination of dioxygen to the Pt central atom, the O–O bond distance is lengthened by 0.13 Å illustrating that the O_2 molecule has been strongly activated. Moreover, the O_2 coordination strengthens the Pt–N bond, probably as a result of the increased π-back bonding effect. The Pt–N bond length is shortened by about 0.05 Å, while the Pt–N bond overlap population increases from 0.070 to 0.081. Interestingly, the significant charge transfer of about 0.40 (0.28) charge units of natural (net atomic) charge from the Pt central atom to coordinated O_2 ligand seems to be the reason for the activation of O_2 upon coordination. Such a π-back bonding effect is supported by the HOMO-4 (at –9.70 eV) shown in Fig. 6a. The computed bond overlap population (BOP) value of

0.053 for the O–O bond of the coordinated O_2 is much lower than the corresponding value of 0.089 of the free O_2 molecule. The total spin density is mainly located on the dioxygen ligand (0.56) and much less on the Pt central atom (0.10) (Fig. 6a). On the other hand, the computed isotropic Fermi contact couplings for O_2 and Pt range from –34.9 to 0.0 MHz.

The migration of one of the O-donor atoms of the coordinated O_2 ligand to the N-donor atom of the NO ligand results in the formation of complex **5** involving a coordinated NO_2 ligand. Noteworthy is the slightly bent structure of complex **5**, the bending angle being 169.5°. The nitrooxoplatinum complex **5** is 33.7 (30.8) kcal/mol more stable than the (dioxygen)nitrosyl platinum complex **4**. Obviously, the O migration is pre-

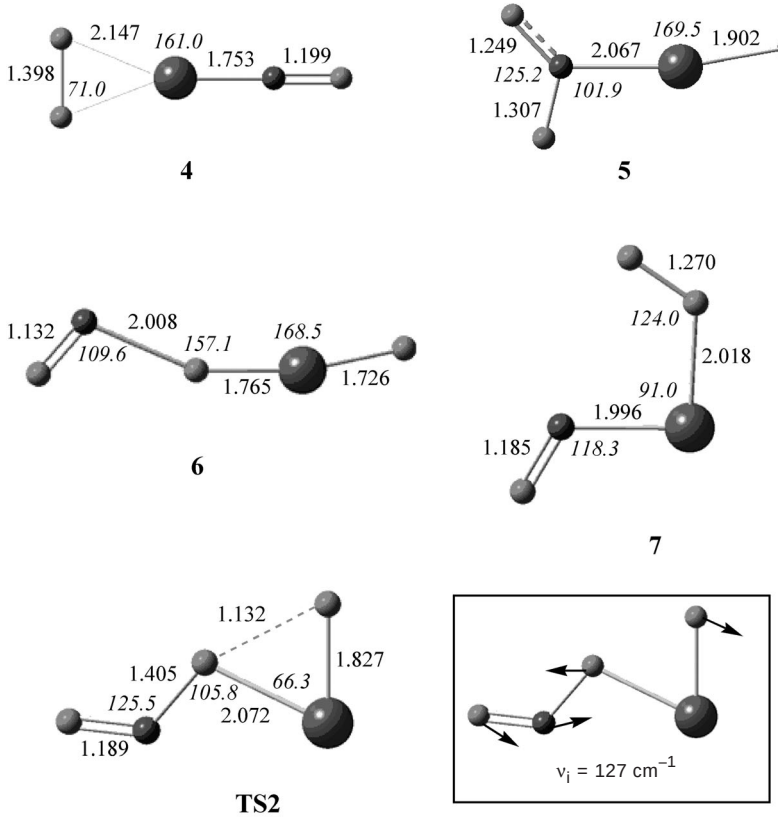

FIG. 5
Equilibrium structures (bond lengths in Å, bond angles in °) of the stationary points located on the PES of the [Pt(NO),O_2] and [Pt(NO),O_2]$^+$ systems

dicted to be an exothermic process. Unfortunately, all attempts to locate on the PES the respective transition state for the migration process were not successful.

In effect, we were able to locate on the PES complex **6**, which involves a η^1-O instead of a η^1-N coordinated NO_2 ligand. Complex **6** could be better described as a loose association of the NO^+ ligand with a PtO_2 species. The computed N···O separation distance (2.008 Å) is much longer than the N–O bond length in the NO_2 ligand (1.25 Å). Moreover, the N–O bond length of 1.132 Å is very close to that of the free NO^+ ligand (1.107 Å) computed at the same level of theory. These observations are also mirrored on the BOP values of the respective bonds. Thus, the N···O BOP value of 0.022 suggests weak interactions, while the N–O BOP value of 0.363 is very close to that of the free NO^+ ligand (0.410). The nature of the weak interactions of the NO^+ ligand with the PtO_2 moiety are clearly described by the nature of the HOMO and LUMO of **6** shown in Fig. 6b. The global minimum on the PES

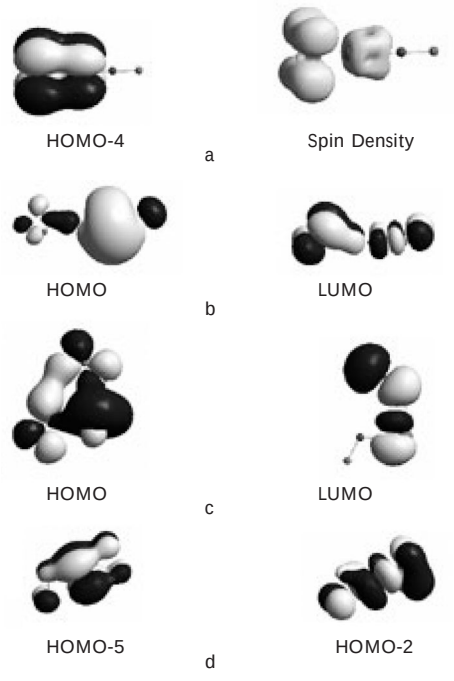

FIG. 6

The HOMO-4 corresponding to π-back bonding and the atomic spin density (isospin surface of 0.002 a.u.) of complex **4** (a), the HOMO and LUMO of complexes **6** (b) and **7** (c), HOMO-5 and HOMO-2 corresponding to π-back bonding to O_2 and NO ligands of complex **8** (d), respectively

of the [$Pt(NO)^+$,O_2] system corresponds to complex **7**, which involves the dioxygen ligand coordinated to the central Pt atom in an end-on bonding mode. The Pt–O bond in **7** is almost perpendicular to the Pt–N bond, the ∠O–Pt–N bong angle being 91.0°. Both the NO and O_2 ligands are coordinated to Pt central atom in a bending mode, the ∠Pt–N–O and ∠Pt–O–O bond angles being 118.3 and 124.0°, respectively. The computed interaction energy of the end-on bonded O_2 ligand in **7** was found to be 49.2 (48.4) kcal/mol. Interestingly, there are weak interactions between the terminal O atom of the O_2 ligand and the N atom of the NO ligand, due to the bonding orbital interactions involved in the HOMO of **7** (Fig. 6c). The π-back bonding effect is less pronounced in the end-on bonded dioxygen compound; the charge transferred from the Pt central atom to dioxygen ligand was found to be about 0.07 (0.14) charge units of natural (net atomic) charge. Because of the weaker π-back bonding effect, the O_2 molecule is activated to a lesser extent upon coordination; the O–O bond length of 1.270 Å is similar to that of the free ligand (1.268 Å). This is also reflected in the computed BOP value (0.081) of the O–O bond, which is exactly the same as that in the free ligand. Finally, the weak interactions between the terminal O atom of the O_2 ligand and the N atom of the NO ligand are expected to support the migration of the O atom to the N atom of the NO ligand. In effect the migration proceeds through the transition state **TS2** (Fig. 5) with an activation barrier of 33.6 kcal/mol. **TS2** is a product-like transition state. The imaginary frequency of **TS2**, ν_i = 127 cm^{-1}, corresponds to movements of all atoms except platinum. The normal coordinate vectors (arrows) of the vibrational mode are shown in Fig. 5.

Finally, the energetic and geometric profile of the reaction of $[Pt(NO)]^-$ with O_2 is depicted schematically in Fig. 7. The coordination of the O_2 ligand to $[Pt(NO)]^-$ affords the mixed-ligand (dioxygen)nitrosylplatinum complex **8**, involving a side-on coordinated dioxygen ligand analogous to the one found in complex **4**. Complex **8** exhibiting a planar configuration is stabilized by 26.9 (26.5) kcal/mol with respect to the dissociation to $[Pt(NO)]^-$ and O_2 in their ground states. However, the interaction of the O_2 ligand with the $[Pt(NO)]^-$ species is much weaker than the interaction with the neutral Pt(NO) species. The computed binding energy of the O_2 ligand to the $[Pt(NO)]^-$ metal-containing fragment amounts only to 26.9 (26.5) kcal/mol. Noteworthy is the side-on coordination mode of the NO ligand in **8** corresponding to a ∠Pt–N–O bending bond angle of 88.9°. The bending ∠Pt–N–O bond angle in the $[Pt(NO)]^-$ species is 122.5°. In complex **8**, an intramolecular O-migration from the O_2 to the NO ligand occurs *via* the transition state **TS3** affording the anionic mixed ligand nitrooxoplatinum

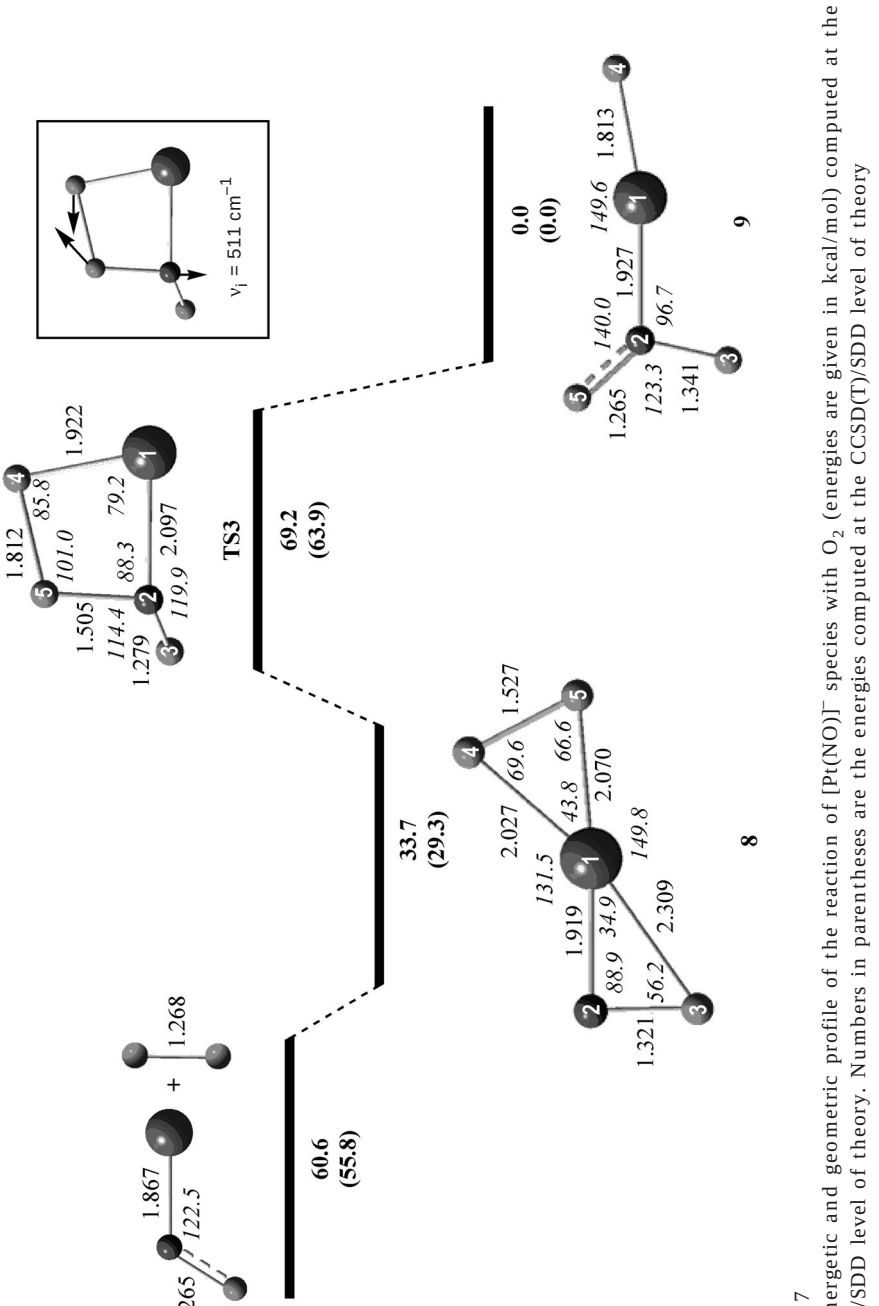

FIG. 7

The energetic and geometric profile of the reaction of $[Pt(NO)]^-$ species with O_2 (energies are given in kcal/mol) computed at the B3LYP/SDD level of theory. Numbers in parentheses are the energies computed at the CCSD(T)/SDD level of theory

complex **9** with a structure analogous to that of the neutral complex **5**. However, the electron attachment affects the structural parameters in complex **9** with respect to complex **5**. Thus the O–Pt–N bending angle is lowered by about 20°, and both the Pt–N and Pt–O bond lengths are shortened by 0.14 and 0.09 Å, respectively. In summary, the transformation of NO to NO_2 in the $[Pt(NO)]^-$ species upon reaction with dioxygen corresponds to an exothermic process; the heat of the reaction is –60.6 (–55.8) kcal/mol and the activation barrier is 35.5 (34.6) kcal/mol. In **TS3**, the coordinated O_2 molecule approaches the N atom of the NO ligand forming a cyclic transition state involving a planar four-membered metallacycle ring. The imaginary frequency of **TS3**, ν_i = 511 cm^{-1}, corresponds primarily to the stretching of the O–O bond. The normal coordinate vectors (arrows) of the vibrational mode are shown in Fig 7. In **TS3**, the O–O bond is lengthened by about 0.29 Å, while the bending Pt–N–O bond angle increases by about 31°. Moreover, there is a remarkable lengthening of the Pt–N bond amounting to 0.18 Å. Upon coordination of the O_2 ligand to Pt central atom of the $[Pt(NO)]^-$ fragment, a significant charge transfer of about 1.13 (0.73) charge units of natural (net atomic) charge from the Pt central atom to dioxygen ligand occurs, which is responsible for the strong activation of the O_2 ligand. Note the elongation of the O–O bond by *ca* 0.26 Å, thus becoming a single O–O peroxo bond (the O–O bond length in H_2O_2 is 1.513 Å at the B3LYP/SDD level). Such a π-back bonding effect is supported by the HOMO-5 (at –3.49 eV) shown in Fig. 6d. The analogous π-back bonding effect with respect to the NO ligand is supported by the HOMO-2 (at –2.57 eV). The computed BOP value of 0.028 for the O–O bond of the coordinated O_2 is much lower than the corresponding value of 0.089 of the free O_2 molecule.

CONCLUSIONS

The use of DFT computational techniques at the B3LYP level of theory, using the SDD basis set, provides a satisfactory description of the geometric, energetic, electronic and spectroscopic properties of the Pt(NO)/Pt(NO_2) redox couple. It was predicted that the neutral Pt(NO) species adopts a bent $^2A'$ ground state, while the cationic $[Pt(NO)]^+$ species a linear $^1\Sigma^+$ ground state. The B3LYP/SDD equilibrium Pt–N bond lengths were found to be 2.016 and 1.777 Å for Pt(NO) ($^2A'$) and $[Pt(NO)]^+$ ($^1\Sigma^+$), respectively, while the Pt–N–O bent angle in Pt(NO) ($^2A'$) is equal to 119.6°. The anionic $[Pt(NO)]^-$ species adopts a bent $^1A'$ ground state with equilibrium Pt–N bond length of 1.867 Å and a Pt–N–O bent angle of 122.5°. The computed

binding energies of the NO, NO^+ and NO^- ligands with Pt(0) were found to be 29.9 (32.8), 69.9 (78.4) and 127.4 (128.7) kcal/mol, respectively, at the B3LYP/SDD and CCSD(T)/SDD (numbers in parentheses) levels of theory. Moreover, the structure of the $[Pt(NO_2)]^+$ component of the $Pt(NO)/Pt(NO_2)$ redox couple and its transformation to $[Pt(NO)]^+$ upon reaction with CO were analysed in the framework of the DFT theory. The coordination of the CO ligand to $PtNO_2^+$ affords the cationic mixed-ligand $[Pt(CO)(NO_2)]^+$ complex, which is stabilized by 66.6 (60.5) kcal/mol, with respect to the separated $[Pt(NO_2)]^+$ and CO species in their ground states. The O-transfer reaction from the coordinated NO_2 to the coordinated CO ligand in the presence of the $[Pt(NO_2)]^+$ species was predicted to be an exothermic process; the heat of the reaction amounts to –85.2 (–80.5) kcal/mol, while the activation barrier is relatively low and amounts to 27.7 (33.0) kcal/mol. Finally, the equilibrium structures of selected stationary points related to the transformation of the NO to NO_2 ligand located on the potential energy surfaces of the $[Pt(NO),O_2]$, $[Pt(NO)^+,O_2]$ and $[Pt(NO)^-,O_2]$ systems were also analysed in the framework of the DFT theory. The computed interaction energies of O_2 with Pt(NO), $[Pt(NO)]^+$ and $[Pt(NO)]^-$ species were found to be 106.9 (105.3), 49.2 (48.4) and 26.9 (26.5) kcal/mol, respectively, at the B3LYP/SDD and CCSD(T)/SDD (numbers in parentheses) levels. The O_2 ligand was found to be coordinated with the Pt central atom in an end-on mode for the $[Pt(NO),O_2]$ and $[Pt(NO)^-,O_2]$ systems and in a side-on mode for the $[Pt(NO)^+,O_2]$ system. The transformation of NO to NO_2 in the $[Pt(NO)]^-$ species upon reaction with dioxygen corresponds to an exothermic process; the heat of the reaction is –60.6 (–55.8) kcal/mol, while the activation barrier amounts to 35.5 (30.2) kcal/mol. Calculated structures, relative stability and bonding properties of all stationary points are discussed with respect to computed electronic and spectroscopic properties, such as charge density distribution and harmonic vibrational frequencies.

REFERENCES

1. a) Murad F.: *Angew. Chem., Int. Ed. Engl.* **1999**, *38*, 1856; b) Furchgott R. F.: *Angew. Chem., Int. Ed. Engl.* **1999**, *38*, 1870; c) Ignaro L. J.: *Angew. Chem., Int. Ed. Engl.* **1999**, *38*, 1882.
2. a) Feelisch M., Stamler J. S. (Eds): *Methods in Nitric Oxide Research*. Wiley, Chichester (U.K.) 1996; b) Ignaro L. J. (Ed.): *Nitric Oxide*. Academic Press, Orlando (FL) 2000; c) Rao D. N. R., Cederbaum A. I.: *Arch. Biochem. Biophys.* **1995**, *321*, 363; d) Fang F. C. (Ed.): *Nitric Oxide and Infection*, Vol. 1 and the following. Kluver Academic/Plenum Publishers, New York 1997.
3. a) Moncada S., Palmer R. M. J., Higgs E. A.: *Pharmacol. Rev.* **1991**, *43*, 109; b) Feldman P. L., Griffith O. W., Stuehr D. J.: *Chem. Eng. News* **1993**, *71*, 26; c) Butler A. R., Williams D. L. H.: *Chem. Soc. Rev.* **1993**, *22*, 223.

4. Noguchi T., Honda J., Nagamune T., Sasabe H., Inoue Y., Endo I.: *FEBS Lett.* **1995**, *358*, 9.
5. Cleeter M. W. J., Cooper J. M., Darley-Usmar V. M., Moncada S., Scapira H. V.: *FEBS Lett.* **1994**, *345*, 50.
6. a) Howard J. B., Rees D. C.: *Chem. Rev. (Washington, D. C.)* **1996**, *96*, 2965; b) Burgess B. K., Lowe D. J.: *Chem. Rev. (Washington, D. C.)* **1996**, *96*, 2983; c) Eady R. R.: *Chem. Rev. (Washington, D. C.)* **1996**, *96*, 3013.
7. a) Zang V., van Eldik R.: *Inorg. Chem.* **1990**, *29*, 4462; b) Pham E. K., Chang S. G.: *Nature* **1994**, *369*, 139.
8. Perry R. A., Miller J. A.: *J. Chem. Kinet.* **1996**, *28*, 217.
9. Monticelly O., Loenders R., Jacobs P. A., Martens J. A.: *Appl. Catal., B* **1999**, *21*, 215.
10. a) Coppens P., Novozhilova I., Kovalensky A.: *Chem. Rev.* **2002**, *102*, 861; b) Andrews L., Citra A.: *Chem. Rev.* **2002**, *102*, 885; c) Mason J., Larkworthy L. F., Moore E.: *Chem. Rev.* **2002**, *102*, 913; d) Hayton T. W., Legzdins P., Sharp W. B.: *Chem. Rev.* **2002**, *102*, 935; e) Ford P. C., Lorkovic I. M.: *Chem. Rev.* **2002**, *102*, 993.
11. a) Ruschel C. K., Nemetz T. M., Ball D. W.: *J. Mol. Struct. (THEOCHEM)* **1996**, *384*, 101; b) Ruschel C. K., Ball D. W.: *High Temp. Mater. Sci. (THEOCHEM)* **1997**, *37*, 63.
12. Thomas J. L. C., Bauschlicher C. W., Jr., Hall M.: *J. Phys. Chem. A* **1997**, *101*, 8530.
13. Blanchet C., Duarte H. A., Salahub D. R.: *J. Chem. Phys.* **1997**, *106*, 8778.
14. Fiedler A., Iwata S.: *J. Chem. Phys.* **1998**, *102*, 3618.
15. a) Andrews L., Zhou M., Ball D. W.: *J. Phys. Chem. A* **1998**, *102*, 10041; b) Kushto G. P., Zhou M., Andrews L. E., Bauschlicher C. W., Jr.: *J. Phys. Chem. A* **1999**, *103*, 1115; c) Zhang L., Zhou M.: *Chem. Phys.* **2000**, *256*, 185.
16. Krim L., Manceron L., Alikhani M. E.: *J. Phys. Chem. A* **1999**, *103*, 2592.
17. Vayner E., Ball D. W.: *J. Mol. Struct. (THEOCHEM)* **2001**, *542*, 149.
18. Erkoc S.: *J. Mol. Struct. (THEOCHEM)* **2001**, *574*, 127.
19. Bauschlicher C. W., Jr., Bagus P. S.: *J. Chem. Phys.* **1984**, *80*, 944.
20. Basch H.: *Chem. Phys. Lett.* **1985**, *116*, 58.
21. Smith G. W., Carter E. A.: *J. Phys. Chem.* **1991**, *95*, 2327.
22. Hrusak J., Koch W., Schwarz H.: *J. Chem. Phys.* **1994**, *101*, 3898.
23. a) Becke A. D.: *Phys. Rev. A: At., Mol., Opt. Phys.* **1988**, *38*, 3098; b) Vosko S. H., Wilk L., Nussair M.: *Can. J. Phys.* **1980**, *58*, 1200; c) Becke A. D.: *J. Chem. Phys.* **1993**, *98*, 5648.
24. Lee C., Yang W., Parr R. G.: *Phys. Rev. B: Condens. Matter* **1988**, *37*, 785.
25. Wadt W. R., Hay P. J.: *J. Chem. Phys.* **1985**, *82*, 5284.
26. Stevens W. J., Basch H., Kraus M.: *J. Chem. Phys.* **1984**, *81*, 6026.
27. Stevens W. J., Kraus M., Basch H., Jasien P. G.: *Can. J. Chem.* **1992**, *70*, 612.
28. Cundari T. J., Stevens W. J.: *J. Chem. Phys.* **1993**, *98*, 5555.
29. a) Nicholas J. B.: *Top. Catal.* **1997**, *4*, 157; b) Koch W. R., Hertwing H.: *Chem. Phys. Lett.* **1997**, *286*, 345; c) Curtis L. A., Raghavachari K., Redfern P. C., Pople J. A.: *Chem. Phys. Lett.* **1997**, *270*, 419; d) Smith D. M., Golding B. T., Radom L.: *J. Am. Chem. Soc.* **1999**, *121*, 9388; e) Chandra A. K., Nguyen M. T.: *Chem. Phys.* **1998**, *232*, 299; f) Nicholas J. B.: *Top. Catal.* **1999**, *9*, 181; g) Arnaud R., Adamo C., Cossi M., Millet A., Vallé Y., Barone V.: *J. Am. Chem. Soc.* **2000**, *122*, 324.
30. Schlegel H. B.: *J. Comput. Chem.* **1982**, *3*, 214.
31. Frisch M. J., Trucks G. W., Schlegel H. B., Scusseria G. E., Robb M. A., Cheeseman J. R., Zakrzewski V. G., Montgomery J. A., Stratmann R. E., Burant J. C., Dapprich S., Millan J. M., Daniels A. D., Kudin K. N., Strain M. C., Farkas O., Tomasi J., Barone V., Cossi M., Cammi R., Mennucci B., Pomelli C., Adamo C., Clifford S., Orchterski J., Petersson G. A.,

Ayala P. Y., Cui Q., Morokuma K., Malick D. K., Rabuck A. D., Raghavachari K., Foresman J. B., Cioslowski J., Ortiz J. V., Stefanov B. B., Liu G., Liashenko A., Piskorz P., Komaroni I., Gomperts R., Martin R. L., Fox D. J., Keith T., Al-Laham M. A., Peng C. Y., Nanayakkara A., Gonzalez C., Challacombe M., Gill P. M., Johnson P., Chen W., Wong M. W., Andres J. L., Head-Gordon M., Replogle E. S., Pople J. A.: *GAUSSIAN98*, Revision A.7. Gaussian Inc., Pittsburgh (PA) 1998.

32. *ChemOffice 97*. Cambridge Scientific Computing, Inc., 875 Massachusetts Ave., Suite 41, Cambridge, MA 02139, U.S.A.
33. Huber K., Herzberg G.: *Constants of Diatomic Molecules*. Van Nostrand Reinhold Co., New York 1979.
34. Walch S. P., Goddard W. A., III: *Chem. Phys. Lett.* **1975**, *33*, 18.
35. Citra A., Andrews L.: *J. Phys. Chem. A* **2000**, *104*, 8160.
36. Zhou M. F., Andrews L.: *J. Phys. Chem. A* **2000**, *104*, 3915.